Observation of plasma array dynamics in 110 GHz millimeter-wave air breakdown

Alan M. Cook,[a] Jason S. Hummelt, Michael A. Shapiro, and Richard J. Temkin
Plasma Science and Fusion Center, Massachusetts Institute of Technology, 167 Albany St., Cambridge, Massachusetts 02139, USA

(Received 25 July 2011; accepted 9 October 2011; published online 27 October 2011)

We present dynamical measurements of self-organizing arrays of plasma structures in air induced by a 110 GHz millimeter-wave beam with linear or circular polarization. The formation of the individual plasmas and the growth of the array pattern are studied using a fast-gated (5–10 ns) intensified camera. We measure the time-dependent speed at which the array pattern propagates in discrete steps toward the millimeter-wave source, observing a peak speed greater than 100 km/s. We observe the expansion of an initially spherical plasma into a disk or an elongated filament, depending on the polarization of the incident beam. The results show good agreement with one-dimensional ionization-diffusion theory and two-dimensional simulations. © *2011 American Institute of Physics*. [doi:10.1063/1.3656980]

Experiments with high-intensity (MW/cm^2) millimeter-wave beams focused in atmospheric-pressure air have observed discharge plasmas with complex dynamics that are unique to this frequency range (30 GHz–1 THz).[1–3] The interaction of the radiation beam with the near-critical-density breakdown plasma, in the absence of the quantum and nonlinear optical effects that dominate laser-plasma interactions, leads to a reflected-field interference pattern with periodicity on the order of the characteristic length for electron diffusion. This allows subsequent breakdowns at the adjacent intensity maxima of the interference pattern to be seeded by the preceding breakdown, causing a self-organizing array-like pattern of plasma formations.[4] Experimental characterization of this phenomenon is important, as the continuing development of mm-wave/THz sources brings new capabilities[5,6] and applications[7,8] for high-power quasi-optical beams that propagate in the atmosphere.

Early breakdown experiments observed a periodic pattern of plasma "filaments," oriented parallel to the incident E-field polarization, that propagates in discrete jumps toward the microwave source.[1,2] Working at 110 GHz (wavelength $\lambda = 2.7$ mm), Hidaka *et al.*[9] observed a two-dimensional (2D) array of such filaments, using steady-state electromagnetic simulations to explain the distinct triangular $\sim\lambda/4$ array spacing. Fast-gated photography showed the sequential pattern formation and estimated its speed at $\sim$10 km/s.

Self-consistent numerical models are able to reproduce many of the experimental results. 1D simulations of the reflection of millimeter waves by a plasma "slab" show the appearance of a new breakdown at the nearest reflected field maximum $\sim\lambda/4$ upstream of the initial plasma, and the rapid subsequent reflection by the new plasma.[4,10] 2D simulations of a linearly-polarized plane wave incident on a plasma spheroid show the elongation of the sphere into a filament due to enhancement of the external electric field at its poles, and the formation of a pattern of filaments.[11–14] Although these simulations closely match experiments, the predicted plasma dynamics have not been measured in this high-frequency, high-intensity regime.

In this letter, we present detailed measurements of the instantaneous dynamics of plasma array patterns in atmospheric air produced by linearly-polarized (LP) and circularly-polarized (CP) 110 GHz millimeter waves. The megawatt-level beam power allows discharge formation in a free volume of gas, with no surfaces or objects nearby. We simultaneously observe the formation of individual plasmas and the discrete axial propagation of the pattern with 20-50 ns temporal resolution over a 3 μs pulse. We measure a pattern propagation speed that decreases by an order of magnitude during the life of the breakdown, from >100 km/s to 10 km/s. The transverse expansion speed of an individual plasma is $\sim$5–10 km/s and shows good agreement with 1D ionization-diffusion theory.[15]

The experimental setup is shown in Fig. 1. A linearly-polarized Gaussian millimeter-wave beam is produced by a 1.5 MW, 110 GHz gyrotron oscillator.[16] The beam is reflected from a metal grating polarizer (10 grooves/cm) that can be rotated to select either linear or circular polarization for the reflected beam. The beam is focused by a high-density polyethylene lens to a peak intensity of 5 MW/cm^2 (1/*e* spot radius $w_0 \approx 4$ mm, peak E field 6 MV/m), causing breakdown in the air near the beam focus. The gyrotron is pulsed at a rate

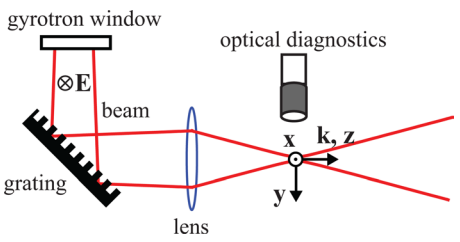

FIG. 1. (Color online) Experimental setup: The breakdown plasma initiates at the origin of the coordinate system at the center of the focused beam waist.

[a]Electronic mail: alancook@mit.edu.

of up to 4 Hz, and the plasma dynamics are observed over many shots using optical diagnostics.

On each shot, a digital camera with slow shutter speed takes a time-integrated photograph capturing the entire breakdown event. An avalanche photodiode detects the onset of optical emission from the breakdown plasma, marking $t = 0$. An intensified CCD camera (ICCD) with a fast shutter speed (5–10 ns) is triggered at a chosen time t during the breakdown. Because the behavior of the breakdown plasma is very repeatable from shot to shot, we can assemble the resulting sequence of fast images into a time-resolved record of an entire breakdown event. The visible emission detected by the ICCD camera is primarily from the $C^3\Pi_u - B^3\Pi_g$ (second positive) system in neutral molecular nitrogen, which we observe with a broadband optical spectrometer. This N_2 system has also been seen to dominate emission in lower-frequency microwave air breakdown on dielectric surfaces.[17] N_2 excitation from the ground state to the $C^3\Pi_u$ state is due to collisions with energetic electrons; since the time between collisions $\tau \lesssim 10^{-12}$ s at atmospheric pressure is much smaller than the time scale of the plasma front motion, we take the excited N_2 front to be an excellent approximation to the position of the plasma electron density front.

Figure 2 shows a subset of the measured sequence for the LP case, taken from hundreds of similar data points. Each frame is a separate breakdown event, with the fast-gated image (orange) overlaid on the corresponding slow image (blue). The envelope of the focused incident beam is shown as a dashed line. The filaments stretch quasi-parallel to the E field polarization ($\hat{x}$), which lies in the plane of the image. When viewed looking along $\hat{x}$, we observe the 2D array pattern described in detail in Ref. 3. When the beam is circularly polarized, the preferred direction is removed, and the plasma expands in both $\hat{x}$ and $\hat{y}$ to form disk-like structures that are azimuthally symmetric (Fig. 3).[18]

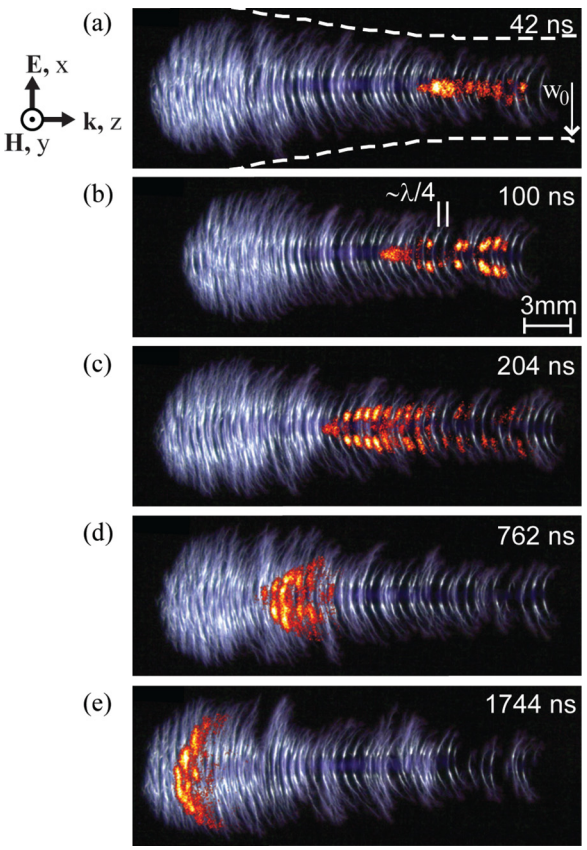

FIG. 2. (Color online) Open-shutter (background image, blue) and fast-gated (overlay, orange) photographs of breakdowns with linearly polarized beam.

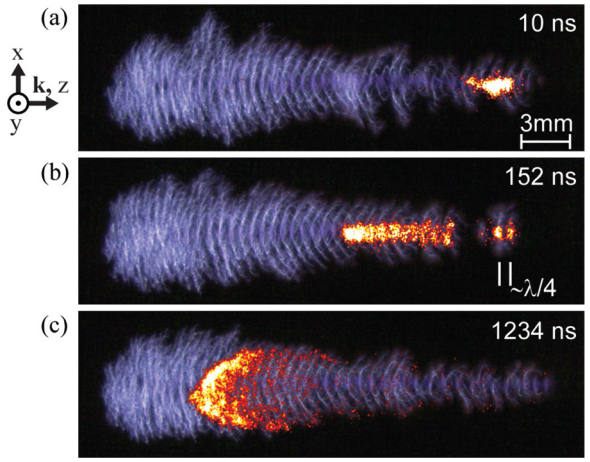

FIG. 3. (Color online) Open-shutter (background image, blue) and fast-gated (overlay, orange) photographs of breakdowns with circularly polarized beam.

It is apparent that each plasma begins as a spheroid on the axis of the Gaussian beam and expands transversely under the influence of the incident field. The axial propagation of the pattern in the $-\hat{z}$ direction is caused by reflection of the incident field and subsequent breakdown at the standing-wave maximum field location $\sim\lambda/4$ upstream. We measure the axial propagation speed v_z by recording the position of the front plasma filament as a function of t, shown in Fig. 4. We see that v_z changes dramatically during the breakdown event, decreasing from >100 km/s to 10 km/s, and is very similar for both polarizations. This decrease in speed is due to the decreasing intensity of the incident Gaussian beam as the plasma moves away from the focus. A logarithmic function is an excellent fit to the position data, indicating an apparent front velocity that is inversely proportional to time.

To measure the growth of an individual plasma formation transverse to the z axis, we record the vertical (in $\hat{x}$) pixel intensity profile at a fixed z position in sequential fast-gated images. We choose a z position located at a newly formed spherical plasma, and follow its growth in time. Fig. 5 shows a sequence of such profiles for a filament

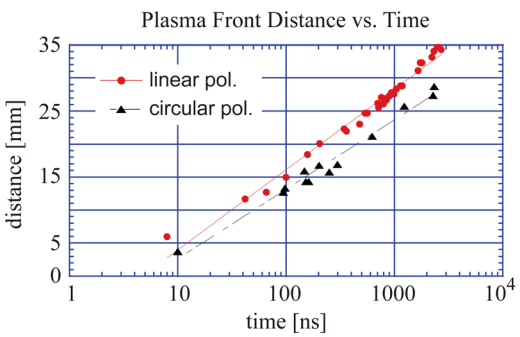

FIG. 4. (Color online) Position of the plasma pattern front vs. camera trigger time t. The lines are logarithmic fits to the data.

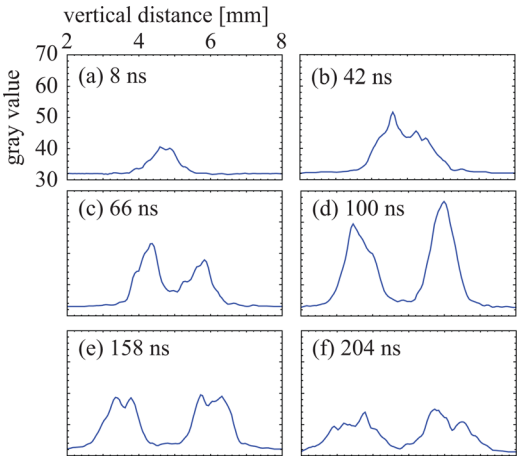

FIG. 5. (Color online) Vertical profiles of pixel intensity at fixed z in fast-gated images of breakdown with linearly polarized beam. Each frame is labeled with camera trigger time t. This sequence follows a filament born around 8 ns (a).

observed starting at 8 ns, in the LP case. The observed radial expansion speed of the plasma front from the axis is $v_\perp \approx 14$ km/s early in the life of the filament and decreases to $\sim$3.5 km/s at later times. In the CP case, $v_\perp \approx 4$ km/s at early times and decreases to $\sim$1 km/s at later times.

The data show that many new breakdowns occur in the time it takes an individual filament to stretch out transversely; for example, in Fig. 2(c), about 10 new filaments have appeared in the time it has taken the earliest filaments to reach full size. This indicates that the incident field is reflected from the plasma early in the life of the filament, allowing a new breakdown to occur while the filament forms. Similar behavior is seen in the CP case. Thus, the self-organization of the pattern is dominated by the part of the plasma near the axis of the incident beam. This is supported by the appearance of a distinct dark channel on the beam axis in the time-integrated photos, which suggests that the incident microwave power is most strongly reflected and absorbed by the center part of the plasma, causing the downstream (earlier) on-axis plasma to extinguish quickly. As the plasma expands away from the beam axis, it does not cut off power to earlier filaments as effectively. This is clearly seen in the fast-gated photos (Fig. 2), which show that the center of each plasma formation disappears within $<$50 ns, while the off-axis part of the plasma persists for $\gtrsim$500 ns. The 1D simulations of similar experimental conditions in Ref. 4 show that the newly formed plasma heavily absorbs power and becomes highly reflecting in $\sim$10 ns. The 2D simulation in Fig. 5 of Ref. 12 shows a similar dark channel in a time-averaged calculation of the electron density.

High-frequency streamer theory describes how a plasma spheroid in an external field distorts into an elongated shape by self-consistently calculating the effects of the changing plasma shape and density on the field.[15] When the plasma approaches critical density, it has a dielectric effect that enhances the field at the edges of the sphere. Depending on the beam polarization, the plasma grows into an elongated ellipsoid (filament) or a flattened ellipsoid (disk). This theory qualitatively explains the observed difference in the plasma geometry in the LP and CP cases. $v_\perp$ is generally lower in the CP case because the field-enhancing effect of the plasma is less pronounced for the flattened disk-like geometry.

We compare the transverse expansion data with simple 1D ionization-diffusion theory, which describes the motion of a plasma ionization front through a neutral gas in an external electric field. The advantage of using this simple theory is that we do not need to assume any unknown parameters, such as the initial electron density or plasma aspect ratio. The speed v_e of the front is found by solving an electron continuity equation, including a source term for ionization due to the millimeter-wave pulse,

$$\frac{\partial n_e}{\partial t} = D_e \nabla^2 n_e + \nu_i n_e, \tag{1}$$

where n_e is the electron density and D_e is the free electron diffusion coefficient at 760 Torr.[19] We assume that D_e is uniform in the region because it depends weakly on the electric field. The net ionization rate ν_i is given by

$$\nu_i = \nu_a \left(\frac{E_{inc}}{E_c}\right)^{\beta} - \nu_a, \tag{2}$$

where $\nu_a = 5 \times 10^4 p$ Hz is the electron-neutral attachment rate in air at pressure p (Torr), E_{inc}/E_c is the ratio of the incident field amplitude to the high-pressure breakdown threshold field $E_c = 3200p$ (V/m),[19] and β is an empirically determined constant ($\beta = 5.33$ for air).[20] Equations (1) and (2) yield a 1D solution for an ionization front traveling at speed[13]

$$v_e = 2\sqrt{D_e \nu_i}, \tag{3}$$

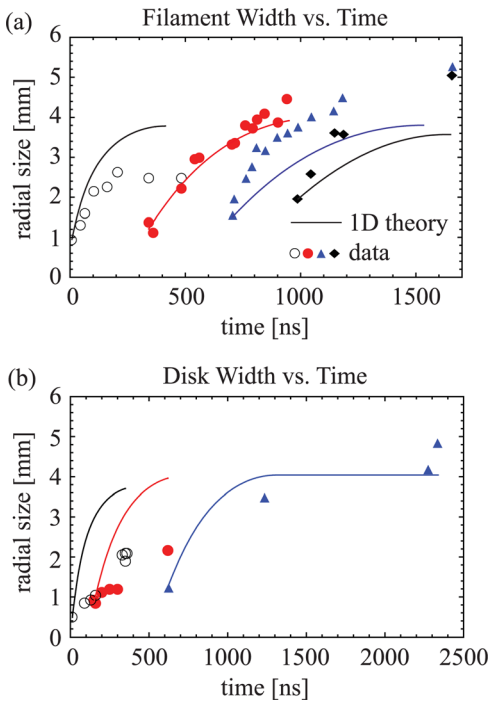

FIG. 6. (Color online) Radial size of (a) filaments (linear polarization) and (b) disks (circular polarization) vs. camera trigger time, t, for plasmas born at different times.

where v_e is independent of the direction of the applied field and does not account for the observed differences in LP and CP plasma expansion speeds.

Fig. 6 shows the measured transverse expansion of plasma filaments born at different times, plotted as the radial size of the plasma versus camera trigger time t, for the LP (filaments, Fig. 6(a)) and CP (disks, Fig. 6(b)) cases. The data are compared with the 1D theory of Eq. (1) using the unperturbed incident beam field $E_{inc}(r,z)$ calculated by Gaussian optics. To calculate the radial size, Eq. (3) is integrated numerically in time, accounting for the Gaussian field variation $E_{inc}(r)$ at a fixed z position. The theory agrees qualitatively with the data, showing that $v_\perp$ is higher closer to the axis of the beam where the incident field intensity is the highest. The calculated expansion stops at larger radii, where E_{inc} is low enough that attachment balances ionization; the observed plasma continues to grow beyond this point due to the field enhancement by the plasma. For the plasma born earliest, before $\sim$200 ns, the data for both polarizations lie well below the theory curve because the growth is slowed by the high reflection/absorption near the beam axis. It is notable that the 1D theory shows reasonable quantitative agreement without any assumed or variable parameters.

These measurements show the dynamics of a self-organized millimeter-wave discharge plasma array and its constituent formations simultaneously. By observing the relative time scales of individual plasma formation (filament or disk) and pattern propagation, we show that the pattern is formed by the early breakdown plasmas near the axis of the beam. Subsequently, the individual plasma growth is effectively decoupled from the pattern formation, driven instead by the incident beam.

The authors thank Y. Hidaka for fabrication of the grating and J. Verboncoeur, A. Vikharev, and M. Gitlin for useful discussions. This work was supported by AFOSR Grant No. FA9550-09-1-0363 on the Basic Physics of Distributed Plasma Discharges.

[1]A. L. Vikharev, V. B. Gildenburg, S. V. Golubev, B. G. Eremin, O. A. Ivanov, A. G. Litvak, A. N. Stepanov, and A. D. Yunakovskii, Sov. Phys. JETP **67**, 724 (1988).
[2]A. L. Vikharev, A. M. Gorbachev, A. V. Kim, and A. L. Kolysko, Sov. J. Plasma Phys. **18**, 554 (1992).
[3]Y. Hidaka, E. M. Choi, I. Mastovsky, M. A. Shapiro, J. R. Sirigiri, and R. J. Temkin, Phys. Rev. Lett. **100**, 035003 (2008).
[4]S. K. Nam and J. P. Verboncoeur, Phys. Rev. Lett. **103**, 055004 (2009).
[5]K. Felch, B. Danly, and H. Jory, Proc. IEEE **87**, 752 (1999).
[6]K. Sakamoto, A. Kasugai, and K. Takahashi, Nat. Phys. **3**, 411 (2007).
[7]Y. Oda, K. Komurasaki, and K. Takahashi, J. Appl. Phys. **100**, 113307 (2006).
[8]V. L. Granatstein and G. S. Nusinovich, J. Appl. Phys. **108**, 063304 (2010).
[9]Y. Hidaka, E. Choi, I. Mastovsky, M. Shapiro, J. Sirigiri, R. Temkin, G. Edmiston, A. Neuber, and Y. Oda, Phys. Plasmas **16**, 055702 (2009).
[10]W. M. Bollen, C. L. Yee, A. W. Ali, M. J. Nagurney, and M. E. Read, J. Appl. Phys. **54**, 101 (1983).
[11]J.-P. Boeuf, B. Chaudhury, and G. Q. Zhu, Phys. Rev. Lett. **104**, 015002 (2010).
[12]B. Chaudhury, J.-P. Boeuf, and G. Q. Zhu, Phys. Plasmas **17**, 123505 (2010).
[13]G. Q. Zhu, J.-P. Boeuf, and B. Chaudhury, Plasma Sources Sci. Technol. **20**, 035007 (2011).
[14]Q. Zhou and Z. Dong, Appl. Phys. Lett. **98**, 161504 (2011).
[15]V. B. Gil'denburg, I. S. Gushchin, S. A. Dvinin, and A. V. Kim, Sov. Phys. JETP **70**, 645 (1990).
[16]E. Choi, A. Cerfon, I. Mastovsky, M. Shapiro, J. Sirigiri, and R. Temkin, Fusion Sci. Technol. **52**, 334 (2007).
[17]G. Edmiston, J. Krile, A. Neuber, J. Dickens, and H. Krompholz, IEEE Trans. Plasma Sci. **34**, 1782 (2006).
[18]S. I. Gritsinin, I. A. Kossyi, and N. M. Tarasova, Sov. Tech. Phys. Lett. **11**, 382 (1985).
[19]A. D. MacDonald, *Microwave Breakdown in Gases* (Wiley, New York, 1966).
[20]W. C. Taylor, W. E. Scharfman, and T. Morita, *Advances in Microwaves* (Academic, New York, 1971), Vol. 7.